International Journal of Pharmaceutics 391 (2010) 284–291

Contents lists available at ScienceDirect

International Journal of Pharmaceutics

journal homepage: www.elsevier.com/locate/ijpharm

Pharmaceutical Nanotechnology

Interactions of lipid-based liquid crystalline nanoparticles with model and cell membranes

Justas Barauskas[a,*], Camilla Cervin[b], Marija Jankunec[a], Marija Špandyreva[a,c], Kristina Ribokaitė[a,c], Fredrik Tiberg[b], Markus Johnsson[b,**]

[a] Institute of Biochemistry, Mokslininkų 12, LT-086 62 Vilnius, Lithuania
[b] Camurus, Ideon Science Park, Sölvegatan 41, SE-223 70 Lund, Sweden
[c] Faculty of Chemistry, Vilnius University, Naugarduko 24, LT-03225 Vilnius, Lithuania

ARTICLE INFO

Article history:
Received 2 November 2009
Received in revised form 18 February 2010
Accepted 1 March 2010
Available online 7 March 2010

Keywords:
Lipid nanoparticles
Liquid crystals
Liposomes
Hemolysis
Interaction kinetics
FRET fluorescence

ABSTRACT

Lipid-based liquid crystalline nanoparticles (LCNPs) are interesting candidates for drug delivery applications, for instance as solubilizing or encapsulating carriers for intravenous (i.v.) drugs. Here it is important that the carriers are safe and tolerable and do not have, e.g. hemolytic activity. In the present study we have studied LCNP particles of different compositions with respect to their mixing behavior and membrane destabilizing effects in model and cell membrane systems. Different types of non-lamellar LCNPs were studied including cubic phase nanoparticles (Cubosome®) based on glycerol monooleate (GMO), hexagonal phase nanoparticles (Hexosome®) based on diglycerol monooleate (DGMO) and glycerol dioleate (GDO), sponge phase nanoparticles based on DGMO/GDO/polysorbate 80 (P80) and non-lamellar nanoparticles based on soy phosphatidylcholine (SPC)/GDO. Importantly, the LCNPs based on the long-chain monoacyl lipid, GMO, were shown to display a very fast and complete lipid mixing with model membranes composed of multilamellar SPC liposomes as assessed by a fluorescence energy transfer (FRET) assay. The result correlated well with pronounced hemolytic properties observed when the GMO-based LCNPs were mixed with rat whole blood. In sharp contrast, LCNPs based on mixtures of the long-chain diacyl lipids, SPC and GDO, were found to be practically inert towards both hemolysis in rat whole blood as well as lipid mixing with SPC model membranes. The LCNP dispersions based on a mixture of long-chain monoacyl and diacyl lipids, DGMO/GDO, displayed an intermediate behavior compared to the GMO and SPC/GDO-based systems with respect to both hemolysis and lipid mixing. It is concluded that GMO-based LCNPs are unsuitable for parenteral drug delivery applications (e.g. i.v. administration) while the SPC/GDO-based LCNPs exhibit good properties with limited lipid mixing and hemolytic activity. The correlation between results from lipid mixing or FRET experiments and the *in vitro* hemolysis data indicates that FRET assays can be one useful screening tool for parenteral drug delivery systems. It is argued that the hemolytic potential is correlated with chemical activity of the monomers in the mixtures.

1. Introduction

Non-lamellar nanoparticles formed by the dispersion of self-assembled lipid liquid crystalline (LC) phases in aqueous solution feature both hydrophilic and hydrophobic domains forming mono- or bicontinuous networks depending on the molecular nature of the lipid or lipid mixture (Larsson, 2000). One key application area of these systems is the use as delivery vehicles for therapeutic and diagnostic agents (Drummond and Fong, 2000; Spicer, 2005; Boyd et al., 2006; Johnsson et al., 2006; Malmsten, 2007; Cervin et al., 2009; Lee et al., 2009; Yaghmur and Glatter, 2009).

Lipids are amphiphilic molecules that can self-assemble into different LC phases (polymorphism), where relatively small alterations in molecular or ambient properties control phase behavior and morphology (Luzzati and Husson, 1962; Larsson et al., 2006). In analogy with liposomal dispersions (liposomes), reversed non-lamellar phase particles can be prepared by dispersion formation in excess aqueous solution in the presence of a stabilizing agent (Barauskas and Nylander, 2008). The most thoroughly studied and characterized system of a non-lamellar phase forming lipid is the glycerol monooleate (GMO) (or monoolein)/water system, that at physiologically relevant temperatures forms a bicontinuous cubic

* Corresponding author. Tel.: +370 5 2729068; fax: +370 5 2729196.
** Corresponding author. Tel.: +46 46 2865745; fax: +46 46 2865739.
E-mail addresses: justas.barauskas@bchi.lt (J. Barauskas), markus.johnsson@camurus.com (M. Johnsson).

0378-5173/$ – see front matter © 2010 Elsevier B.V. All rights reserved.
doi:10.1016/j.ijpharm.2010.03.016

phase in excess aqueous solution (Lutton, 1965; Hyde et al., 1984; Qiu and Caffrey, 2000). The GMO cubic phase may be fragmented into stable aqueous nanoparticle dispersions by the use of a stabilizing fragmentation agent such as Pluronic F127, a tri-block co-polymer of ethylene oxide and propylene oxide (EO–PO–EO) (Ljusberg-Wahren et al., 1996; Gustafsson et al., 1997; Barauskas et al., 2005a). Intriguing internal 3D nanostructures of the GMO-based cubic phase nanoparticles have been observed and characterized by, e.g. cryogenic transmission electron microscopy (cryo-TEM) (Barauskas et al., 2005a,b). Several publications dealing with the application of GMO-based particle dispersions in drug delivery have also emerged during the past decade or so (Um et al., 2003; Leesajakul et al., 2004).

More recently it has been shown that all well-known non-lamellar reversed lipid liquid crystals (bicontinuous cubic, "sponge", hexagonal, and micellar cubic) can be dispersed into colloidal nanoparticles when using suitable lipid combinations and preparation techniques (Barauskas et al., 2005b, 2008; Johnsson et al., 2005; Barauskas and Nylander, 2008; Salentinig et al., 2008). Although the spectrum of such colloidal lipid self-assembly structures for drug delivery application appears exhaustive in theory, in practice cost, safety and regulatory demands impose a significant restriction in which systems that can be used. There are only a limited number of lipids and surfactants with prior use in pharmaceutical products which realistically can be applied as parenteral drug delivery agents without performing extensive toxicology studies (Strickley, 2004; Chen, 2008).

In recent trials we have introduced lipid combinations based on soy phosphatidylcholine (SPC), glycerol dioleate (GDO) and polysorbate 80 (P80) as a new alternative for parenteral drug delivery. This system has been designed specifically for the preparation of stable non-lamellar LCNPs (Johnsson et al., 2006; Cervin et al., 2009). A pre-requisite for a parenteral delivery system is low or negligible hemolytic activity. Although the phase behavior and structural features of some non-lamellar lipid dispersions are rather well investigated, a good understanding of interaction aspects between such delivery vehicles and blood cell or model membranes is still lacking. Only a few recent studies provide a link between physical and chemical properties of non-lamellar lipid nanoparticles and their interaction features with phospholipid-based model membranes (Vandoolaeghe et al., 2009a,b).

In the present study we show that the hemolytic activity of different nanoparticle dispersions, i.e. the interaction with the red blood cells (RBCs), is strongly dependent on both the lipid nature and the overall composition. For this purpose, we studied the hemolytic activity of different cubic, hexagonal and "sponge" liquid crystalline nanoparticles. Dispersions based on the following lipid compositions have been investigated: GMO/F127, GMO/P80, SPC/GDO/P80, SPC/GDO/GMO/P80, diglycerol monooleate (DGMO)/GDO/F127 and DGMO/GDO/P80. The latter system was recently introduced as a novel self-dispersing non-lamellar phase forming system with applicability mainly to non-parenteral drug delivery (Barauskas et al., 2006).

To further understand the mechanism of hemolysis, fluorescence energy transfer (FRET) measurements on lipid mixing were performed to investigate the kinetics of lipid transfer between model cell membranes (in the form of multilamellar SPC liposomes) and the non-lamellar nanoparticles of different lipid compositions.

2. Materials and methods

2.1. Materials

Excipients used in the experiments were soy phosphatidylcholine (SPC) (S100 from Lipoid GmbH, Ludwigshafen, Germany), with the major components phosphatidylcholine (95.7%), triglycerides (1.5%) and lysophosphatidylcholine (1.0%); glycerol dioleate (GDO) (Danisco, Aarhus, Denmark), containing diglycerides (94.0%), monoglycerides (0.8%) and triglycerides (4.9%); glycerol monooleate (GMO) (Danisco, Aarhus, Denmark), containing monoglycerides (95.0%) and diglycerides (4.1%); diglycerol monooleate (DGMO) (Danisco, Denmark), containing diglycerol monoester (87.0%), glycerol monoester (2.0%) and free glycerol and polyesters (5.2%); polyoxyethylene (20) sorbitan monooleate (polysorbate 80, P80) (Croda, U.K.); and poly(ethylene oxide) (PEO)–poly(propylene oxide) (PPO)–poly(ethylene oxide) tri-block co-polymer (BASF Svenska AB, Helsingborg, Sweden) with the trade name Pluronic® F127 and approximate formula of $EO_{98}PO_{57}EO_{98}$ (average molecular weight of 12,600 g/mol). N-(7-nitrobenz-2-oxa-1,3-diazol-4-yl)-1,2-dihexadecanoyl-sn-glycero-3-phosphoethanolamine, triethylammonium salt (NBD-PE) and Lissamine™ rhodamine B 1,2-dihexadecanoyl-sn-glycero-3-phosphoethanolamine, triethylammonium salt (*N*-Rh-PE) were obtained from Invitrogen (Carlsbad, CA). Dioleoylphosphatidylethanolamine–poly(ethylene glycol) 2000 (DOPE–PEG(2000) or PEG-lipid) was obtained from Avanti Polar Lipids (Alabaster, Al). All other solvents and reagents were of analytical grade and were used as received. Milli-Q purified water was used for all experiments.

2.2. Preparation of lipid-based liquid crystalline nanoparticles (LCNPs)

Non-aqueous SPC/GDO/P80 and SPC/GDO/GMO/P80 pre-formulations were prepared by combining appropriate amounts of constituents with ethanol (10 wt% ethanol) followed by mixing overnight at room temperature on a roller mixer. Aqueous LCNP dispersions (5 wt% of lipid) were prepared by adding appropriate amount of pre-formulation to pure water (or to 5 wt% glucose solution for use in the hemolysis assay). Samples were then immediately sealed, hand-shaken and left to vortex for 48–72 h on a mechanical mixing table at 180–400 rpm and room temperature (RT). Heat treatment of dispersions was performed where indicated in order to improve dispersion properties in terms of reducing the amount of meta-stable vesicular aggregates. Heat treatment of the mechanically shaken dispersions was performed using a bench-type autoclave (CertoClav CV-EL, Certoclav Sterilizer GmbH, Traun, Austria) operated at 125 °C and 1.4 bar during 20 min. After the heat treatment, the samples were allowed to cool to RT. Preparation procedures of aqueous GMO/F127, GMO/P80, DGMO/GDO/F127 and DGMO/GDO/P80 LCNP dispersions are described elsewhere (Barauskas et al., 2005a, 2006; Johnsson et al., 2005).

2.3. Preparation of LCNP labeled with fluorescent lipids

0.4 mg of NBD-PE and 0.5 mg of *N*-Rh-PE were dissolved in 1.25 ml of a chloroform/ethanol (1/4, v/v) mixture to final concentrations of 0.335 and 0.300 mM, respectively. A stock solution with an equimolar ratio of the fluorescent phospholipids (8 μM) was prepared by adding 0.24 ml of the NBD-PE and 0.27 ml of the *N*-Rh-PE solution to 19.49 ml of ethanol. In order to label the LCNP with fluorescent phospholipids, appropriate amounts (80–150 μl) of stock solution of the equimolar mixture of NBD-PE and *N*-Rh-PE were mixed with 6 ml of LCNP dispersions (0.003 wt% with respect to lipid) and left to equilibrate for 48 h at RT under mild stirring before the measurements. 48 h was the time required to reach steady-state fluorescence. All FRET measurements were performed with freshly prepared LCNP dispersions labeled with the fluorescent lipids.

Table 1
Results from the hemolysis assay of LCNPs with different lipid compositions mixed with fresh whole blood from rat *in vitro* and particle size data. Hemolysis and particle size data are also provided for the aqueous solution of F127 and P80.

Lipid weight ratio (wt%)				Fragmentation agent (wt% with respect to lipid)		Particle size distribution		Hemolysis (%) ($n \geq 3$)	
GMO	DGMO/GDO	SPC/GDO	SPC/GDO/GMO	P80	F127	*d* (nm)	PdI	Mean	SD
100					10	196	0.11	120	14
100					15	199	0.17	114	10
100					20	204	0.17	116	3.4
100					25	206	0.23	114	22
100					30	186	0.26	114	32
100				20		339	0.22	122	16
	50/50				10	154	0.14	1.5	0.2
	50/50			7.5		141	0.14	1.4	0.2
	50/50			15		130	0.16	2.2	0.6
	50/50			20		138	0.21	1.9	0.2
	50/50			30		153	0.23	1.5	0.2
		70/30		20		160	0.17	0.0	0.0
		60/40		20		148	0.18	0.0	0.1
		50/50		20		125	0.20	0.0	0.1
		40/60		20		116	0.20	0.1	0.1
		30/70		20		102	0.24	0.1	0.2
		20/80		20		105	0.22	0.1	0.2
		10/90		20		116	0.20	0.1	0.2
			40/30/30	20		146	0.17	1.9	2.1
			40/24/36	20		141	0.21	1.9	2.1
			40/18/42	20		152	0.13	2.3	2.3
			40/12/48	20		191	0.17	3.3	2.6
			40/6/54	20		236	0.24	7.1	3.3
			40/0/60	20		226	0.26	14	5.7
				100		11.3	0.11	6.6	1.4
					100	24.4	0.27	0.0	0.0

2.4. Preparation of coarse multilamellar liposome dispersion and unilamellar liposomes

Coarse dispersions of multilamellar liposomes were prepared by adding 2.25 g of SPC to 47.75 ml 0.9 wt% NaCl solution. The samples were immediately sealed, hand-shaken and left to vortex for 48–72 h on a mechanical mixing table at 180 rpm and RT. The resulting coarse dispersions of multilamellar liposomes were characterized by a mono-modal size distribution and a mean particle size of 1.3 μm (polydispersity index (PdI) was 0.23).

Unilamellar liposomes comprising SPC or SPC/DOPE–PEG(2000) (PEG-lipid) were prepared by dissolving the lipid or lipid mixture in chloroform followed by evaporation of the solvent under vacuum to form dry lipid films. Hydration of the lipids was performed in 0.9 wt% NaCl solution by repeated freeze–thawing (freezing in liquid nitrogen and thawing in water bath at 50 °C) with intermittent vortex mixing. The dispersions were thereafter extruded through 2 stacked polycarbonate filters of pore size 400 nm 15 times using a LIPEX extruder (Northern Lipids Inc., Burnaby, Canada) to form unilamellar liposomes. The lipid dispersions were then diluted as required for the FRET experiments (see below).

2.5. Particle size measurements

Particle size distributions were measured using a Zetasizer Nano ZS dynamic light scattering instrument (Malvern Instruments Ltd., Worcestershire, U.K.) at 25 °C. The prepared aqueous dispersions were diluted to 1 wt% lipid. Autocorrelation functions were analyzed using Malvern's General Purpose model as supplied in the instrument software. The particle size distributions were characterized by the mean particle size (intensity averaged) and the polydispersity index.

2.6. FRET fluorescence measurements

All FRET fluorescence lipid mixing experiments were performed using LS 55 Fluorescence Spectrometer (PerkinElmer, Waltham, MA). In this study, an assay based on NBD-rhodamine energy transfer, detected as *N*-Rh-PE emission at 580 nm resulting from NBD-PE excitation at 463 nm, was utilized (Struck et al., 1981). Briefly, 2 ml of prepared LCNPs (0.003 wt% with respect to lipid) labeled with 1 mol% of fluorescent phospholipids (0.5 mol% of *N*-Rh-PE and 0.5 mol% of NBD-PE) were added to 1 cm path length quartz cuvettes and mixed with 13 μL 4.5 wt% SPC multilamellar liposomes to a final LCNP/liposomes weight ratio of 1/10 (wt/wt). The resulting fluorescence emission decays were registered at RT at 580 nm for 30 min. All decay curves were corrected for background intensity (scattering) and normalized.

2.7. Hemolysis

Fresh whole blood (heparinized) from rat was mixed with lipid dispersions, prepared as described above (5 wt% total lipid dispersed in an aqueous medium containing 5 wt% glucose), or controls in a ratio of 1:1 (v/v) (total volume of 1 ml). 5 wt% glucose in water for injection (WFI) and 2 wt% Triton X-100 (surfactant) in WFI were used as negative and positive controls, respectively. Samples were incubated at 37 °C with gentle rotation at 200 rpm on a shaking table during 1 h, after which they were centrifuged at 2000 × *g* during 10 min. Supernatants were treated with aqueous 10 wt% Triton X-100 solution in a ratio of 1:4 (v/v) (total volume of 200 μl) to prevent false positive results originating from the turbidity of the lipid dispersions. Absorbance of the Triton X-100 treated supernatant was determined spectrophotometrically in a 96-well microtiterplate at 540 nm. Hemolysis was reported as % of positive control (100% hemolysis) according to $(Abs_{sample} - Abs_{neg})/(Abs_{pos} - Abs_{neg}) \times 100$.

3. Results and discussion

The main objective was to study the relation between some of the key properties of the lipid-based drug delivery carriers and the interactions with model and cell membranes. The ultimate goal is to

achieve a better understanding of the structural/functional carrier properties and the relation to *in vivo* properties such as toxicity and stability in systemic circulation. The work may also help in designing carrier vehicles for specific administration routes, such as parenteral drug administration. To this end, *in vitro* hemolysis data were complemented with the lipid mixing behavior characteristics of different non-lamellar lipid-based liquid crystalline nanoparticles (LCNPs) with model phospholipid liposomes, as assessed by FRET measurements.

3.1. Hemolytic effects of LCNPs

The first part of this work was focused on determination of the hemolytic effects of LCNPs of different lipid and polymer compositions on fresh whole blood from rat *in vitro*. Cubic phase dispersions based on GMO/F127 and GMO/P80 at different lipids to polymers (surfactant) weight ratios (90/10, 85/15, 80/20, 75/25, and 70/30) were prepared. As shown in Table 1, despite different amounts of stabilizing polymer all GMO/F127 based cubic LCNPs showed massive hemolysis, within the range of 117–137% relative to positive control. Exchanging the F127 (20 wt% with respect to GMO) for a different fragmentation agent, P80 (20 wt%, with respect to GMO), resulted in similar results (136% hemolysis), indicating no effect of the nature of the fragmentation agent on the hemolytic activity of GMO-based dispersions. The results clearly indicate the limited applicability of the well-known GMO-based dispersions in pharmaceutical products for i.v. administration.

Hemolytic effects of hexagonal and "sponge" type LCNPs based on mixtures of DGMO/GDO stabilized with F127 (10 wt%, with respect to lipid mixture) and P80 (7.5, 15, 20, and 30 wt% with respect to lipid mixture) were also investigated. As seen from the results presented in Table 1, despite different structural organizations and natures of the stabilizing/fragmentation agent and its concentration, all DGMO/GDO-based dispersions showed very similar and quite small degree of the hemolytic activity in the order of 1–2%.

In our recent studies we have introduced new lipid combinations with applicability for i.v. administration, based on mixtures of SPC/GDO/P80 that form stable and structurally well-defined non-lamellar LCNP dispersions in aqueous media (Johnsson et al., 2006; Cervin et al., 2009). A number of dispersions stabilized with the same concentration of P80 but at different SPC/GDO weight ratios (70/30, 60/40, 50/50, 40/60, 30/70, 20/80, and 10/90) were prepared and tested (Table 1). The results showed essentially no hemolytic activity relative to positive control for either of the dispersions.

Interesting results were obtained with the quaternary SPC/GDO/GMO/P80 dispersion system, where GDO was gradually exchanged for GMO to finally obtain a SPC/GMO/P80 mixture (Table 1 and Fig. 1). The results showed a gradual increase in hemolytic activity from 0.2% (GDO/GMO; 100/0 wt/wt) to 18% when GDO within the LCNP dispersions, was fully replaced by GMO (GDO/GMO; 0/100 wt/wt). The observed behavior of the SPC/GDO/P80 LCNP dispersions in the presence of the highly hemolytically active GMO shows that SPC/GDO/P80 based dispersions can accommodate considerable amounts of monoglyceride (or GMO) "impurities" and still possess low hemolytic activity.

To complement the above data on the different LCNP formulations, the hemolytic effect of both stabilizing polymer (F127) and surfactant (P80) solutions was also investigated. Micellar solutions of 1 wt% P80 and 1 wt% Pluronic F127 were thus prepared and these resulted in hemolysis of 7% and 0%, respectively. Thus, P80 *per se* displays a moderate hemolytic activity when dissolved alone in aqueous solution, as also described elsewhere (Miwa et al., 1998), whereas Pluronic F127 alone appears inert with respect to hemolysis. It is worth noting that 20 wt% P80 with respect to lipid was used for the SPC/GDO/P80 LCNP dispersions (Table 1) and

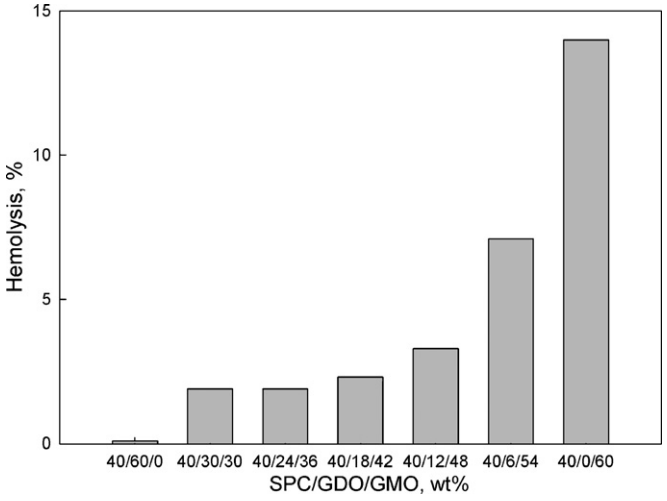

Fig. 1. Hemolysis of rat whole blood induced by lipid LCNP dispersions based on SPC/GDO/GMO/P80 at different SPC/GDO/GMO ratios (40/60/0, 40/30/30, 40/24/36, 40/18/42, 40/12/48, 40/6/54 and 40/0/60). The P80 concentration was in all cases 20 wt% with respect to the other lipid components (see also Table 1). Note the practical absence of hemolysis for the SPC/GDO/P80 dispersion.

that the dispersions of 5 wt% total lipid (mixed 1/1 vol/vol with rat whole blood) as used in the hemolysis experiments therefore corresponds to a total P80 concentration of 1 wt%. Thus, when mixed with SPC/GDO, P80 does not induce any measurable hemolysis, i.e. the activity of P80 was significantly reduced in the mixture compared with the pure aqueous P80 solution. A similar effect was observed with DGMO/GDO/P80 LCNP dispersions. Altogether, the results from hemolysis experiments clearly indicate that hemolytic effects of various non-lamellar LCNP dispersions are mostly driven by the nature of lipid molecules and specific lipid composition but not by the stabilizing polymer (F127) or surfactant (P80).

3.2. FRET fluorescence of LCNP mixing with phospholipid liposomes

The second part of this work was focused on determination of the mixing behavior aspects of different LCNPs with soy phosphatidylcholine (SPC) multilamellar liposomes. FRET experiments were performed by entrapping fluorescent probes (0.5 mol% NBD-PE and 0.5 mol% *N*-Rh-PE) within the dispersed LCNPs, allowing the labeled LCNPs to mix with SPC liposomes, and following fluorescence emission decays with time for 30 min at 580 nm. The obtained fluorescence decay curves were background corrected (intensity data from mixing SPC liposomes with LCNP dispersions without fluorescent probes were subtracted), and normalized (initial intensity was set to 100%). Additionally, all LCNP dispersions were tested to make sure that the fluorescence intensity of the entrapped fluorescence probes did not spontaneously decrease, e.g. due to photo-bleaching, during the timescale of the mixing experiment. To mimic *in vivo* conditions as closely as possible, all FRET mixing experiments were deliberately performed at a LCNP/SPC liposomes weight ratio of 1/10 (wt/wt), i.e. the excess of multilamellar liposomal structures used in the FRET studies would mimic the situation of a systemic dilution of injected LCNPs with an excess of cell membranes present.

Fig. 2 shows the FRET kinetic data obtained from the interaction of GMO/F127, DGMO/GDO/P80, and SPC/GDO/P80 LCNPs with SPC liposomes. As indicated by the fluorescence intensity kinetic decays, GMO-based dispersions showed the highest interaction activity (Fig. 2a). In the presence of SPC liposomes, fluorescence intensities decayed to about 20% of its initial values within the first 30 min of the mixing experiment. This indicates that the average

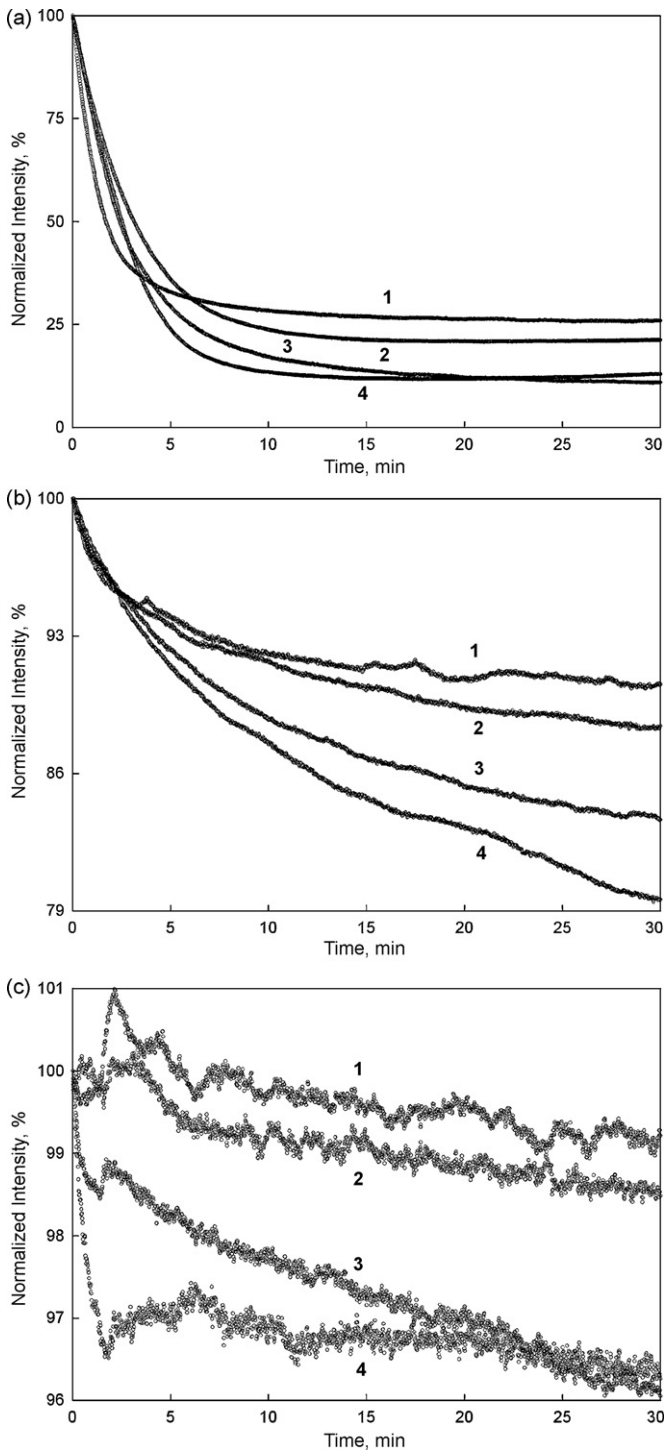

Fig. 2. FRET fluorescence intensity decays upon mixing of SPC multilamellar liposomes with fluorescently labeled (NBD-PE and *N*-Rh-PE) (a) GMO/F127 LCNPs at different GMO-to-polymer weight ratios: 70/30 (1), 80/20 (2), 90/10 (3), and 75/25 (4); (b) DGMO/GDO/P80 LCNPs at different lipid (DGMO + GDO)/P80 weight ratios: 80/20 (1), 70/30 (2), 85/15 (3), and 92.5/7.5 (4); and (c) SPC/GDO/P80 LCNPs at different SPC/GDO weight ratios: 70/30 (1), 50/50 (2), 30/70 (3), and 10/90 (4). The excitation wavelength was 463 nm and the emission intensity was recorded at 580 nm.

distance between the fluorescence probes entrapped within the GMO/F127 dispersions rapidly increased, as a result of fast interaction kinetics and lipid mixing of LCNPs with SPC liposomes. As also seen from Fig. 2a, there was no lipid mixing behavior dependence on the amount of F127 used to stabilize the GMO-based dispersions.

"Sponge" type LCNP dispersions based on DGMO/GDO/P80 mixtures showed moderate interaction with SPC liposomes (Fig. 2b). In this case, fluorescence intensities decayed to about 85% of initial values. Note that the fluorescence intensity decays showed a dependence on the amount of P80 used to stabilize the dispersions. DGMO/GDO/P80 dispersions prepared at lipid/P80 weight ratios of 70/30 and 80/20 decayed only about 10% of the original fluorescence intensity, whereas the dispersions prepared at lipid/P80 weight ratios of 85/15 and 92.5/7.5 decayed 16 and 20%, respectively. In other words, increased amount of P80 prevented, to some extent, the interaction resulting in lipid mixing of such "sponge" type LCNP dispersions with SPC bilayers. In a recent study we have shown that the internal nanostructure of the DGMO/GDO/P80 LCNPs depends on the concentration of P80 (Barauskas et al., 2006). That is, increasing amount of P80 thickens the outer "sponge" phase layer of the nanoparticles in which P80 molecules are preferably located. Therefore, the increasing amount of P80 within the nanoparticles likely provides some additional degree of steric stabilization and restricts fusion/interaction with SPC liposomes. A moderate interaction effect with SPC liposomes was also observed for hexagonal type LCNPs based on the mixture of DGMO/GDO stabilized with F127 (10 wt% with respect to lipid mixture). In this case, the fluorescence intensity decayed to about 70% of its initial value (data not shown).

As seen from the data presented in Fig. 2c, aqueous SPC/GDO/P80 dispersions showed a very low degree of interaction with SPC liposomes. Irrespective of SPC/GDO weight ratios (from 70/30 to 10/90) in the dispersion preparations, only a few percent of the initial fluorescence intensity was lost, indicating practically no lipid mixing with SPC bilayers.

Fig. 3 shows the FRET kinetic data obtained from the interaction of quaternary SPC/GDO/GMO/P80 LCNPs with SPC liposomes. The above data (Fig. 2a) clearly showed that GMO can be characterized as highly "fusogenic" with respect to lipid mixing/interaction with SPC liposomes. Indeed, a gradual exchange of GDO for GMO resulted in increased lipid mixing as indicated by the decrease in fluorescence intensity in Fig. 3. When GDO was fully replaced by GMO, the dispersions showed a moderate interaction with SPC liposomes, as fluorescence intensity decayed to about 70% of the initial value.

To gain insight into interaction features between non-lamellar LCNP dispersions and SPC multilamellar liposomes additional calibration experiments were performed. To roughly estimate the lipid bilayer dilution during the mixing process, experiments were performed by measuring the emission intensity at 580 nm at different fluorescent lipid concentrations (total amount of NBD-PE + *N*-Rh-PE) within the LCNPs. This procedure allows an approximate lipid mixing degree calculation, i.e. to correlate the relative emission decay from the kinetic experiments with the dilution of the fluorescence probes. The results obtained for the three different LCNP dispersion systems, GMO/F127, DGMO/GDO/P80 and SPC/GDO/P80, are summarized in Fig. 4. As expected, the calibration curves showed a near linear decrease in fluorescence intensity with decreasing fluorescence probe concentration. However, especially at low fluorescence probe concentration, the dependencies for the three LCNP dispersions differed slightly. For example, with the SPC/GDO-based LCNP dispersion the fluorescence intensity decreased faster with decreasing probe concentration as compared to the GMO/F127 LCNPs (Fig. 4). This observation is most likely related to the different LCNP nanostructural organizations and different localizations and energy transfer features between the fluorescence probes within the respective lipid nanoparticle.

More importantly, calibration curves presented in Fig. 4 enable rough estimations of the actual mass transfer in the obtained lipid mixing kinetic data presented in Figs. 2 and 3. Thus, upon mixing of GMO/F127 LCNP dispersions with SPC liposomes, the fluores-

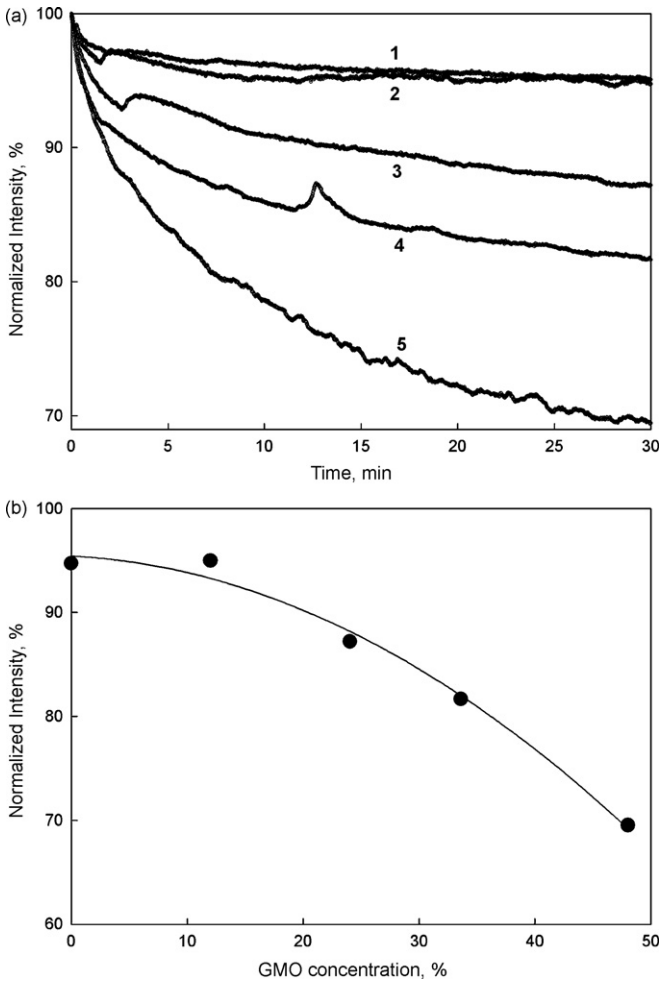

Fig. 3. (a) FRET fluorescence intensity decays upon mixing of SPC multilamellar liposomes with fluorescently labeled (NBD-PE and *N*-Rh-PE) SPC/GDO/GMO/P80 LCNPs at different SPC/GDO/GMO weight ratios: 40/45/15 (1), 40/60/0 (2), 40/30/30 (3), 40/18/42 (4), and 40/0/60 (5). (b) Dependence of the FRET fluorescence intensity on GMO concentration within SPC/GDO/GMO/P80 LCNPs (concentration expressed as wt% of total composition) after 30 min of mixing with SPC multilamellar liposomes. The excitation wavelength was 463 nm and the emission intensity was recorded at 580 nm.

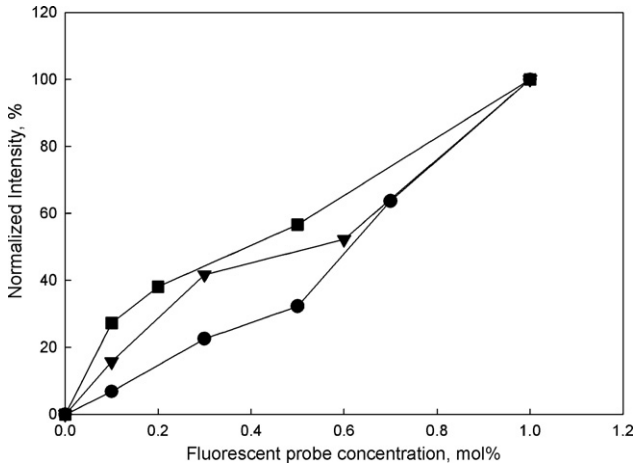

Fig. 4. Dependence of the FRET fluorescence intensity on total NBD-PE + *N*-Rh-PE concentration entrapped within GMO/F127 (squares), DGMO/GDO/P80 (triangles), and SPC/GDO/P80 (circles) LCNP dispersions. The excitation wavelength was 463 nm and the emission intensity was recorded at 580 nm.

cence intensities decayed to about 20% of the initial value (Fig. 2a), indicating a very fast lipid mixing corresponding to more than 10 times dilution of the fluorescence probes within the nanoparticles (Fig. 4). Taking into account that experiments were performed at an LCNP/SPC liposome weight ratio of 1/10, it may be concluded that within 30 min, GMO-based LCNPs and SPC liposomes are totally mixed. In contrast, SPC/GDO/P80 LCNPs showed a very limited interaction with SPC liposomes, indicating almost no lipid exchange and practically no dilution of the fluorescence probes. "Sponge" type (DGMO/GDO/P80 based) LCNPs possessed moderate mixing behavior with SPC, corresponding to a limited mass transfer of approximately 1.2 times dilution of the fluorescence probes.

Taken together, there is a relatively good correlation between the determined *in vitro* hemolytic effects of different LCNPs on RBCs and their mixing behavior with SPC liposomes. As shown in the hemolysis experiments, GMO-based LCNPs display massive hemolysis when mixed with fresh whole blood from rat. Correspondingly, a fast and near complete lipid mixing was observed in FRET experiments with SPC liposomes. SPC/GDO/P80 dispersions, on the other hand, were found to be non-hemolytic and correspondingly the FRET experiments indicated almost no lipid mixing with SPC liposomes.

It is interesting to note the dramatic effect of GMO on both lipid mixing and hemolysis. The critical aggregation concentration (cac) or critical micelle concentration (cmc) of GMO has been determined to be approximately 4×10^{-6} M (Ho and Storch, 2001) and GMO has a much higher monomer activity compared with SPC and GDO that have estimated cacs (or cmcs) in the 10^{-9} to 10^{-10} M range (Tanford, 1991). When GMO is mixed with SPC/GDO, hemolysis and lipid mixing decrease markedly compared with the pure GMO system, but increase gradually with the fraction of GMO in the lipid mixture (Figs. 1 and 3). These effects can be explained by lowering the GMO monomer activity in the mixture. Assuming ideal mixing, one can roughly calculate the cac (cmc) for the lipid mixture, e.g. for the mixtures displayed in Table 1. Taking as an example the SPC/GMO/P80 32/48/20 wt% mixture, with cac (or cmc) values of 10^{-9} M, 4×10^{-6} M and 6×10^{-6} M (Thorsteinsson et al., 2005), for SPC, GMO and P80, respectively, and using Eq. (1) (where α_i and cmc_i are the *i*th component mole fraction and cmc, respectively), the mixed cmc is estimated to approximately 5×10^{-9} M.

$$\frac{1}{\mathrm{cmc}_{\mathrm{mixed}}} = \sum_i \left(\frac{\alpha_i}{\mathrm{cmc}_i} \right). \quad (1)$$

Having established the mixed cmc in the nanomolar range, thus showing that at all experimental conditions used herein there will be lipid aggregates/particles present, the monomer concentration of GMO may be estimated by using Eq. (2) and assuming ideal mixing:

$$C_{\mathrm{GMO}}^{\mathrm{monomer}} = X_{\mathrm{GMO}} \times \mathrm{cmc}_{\mathrm{GMO}}, \quad (2)$$

where X_{GMO} and $\mathrm{cmc}_{\mathrm{GMO}}$ are the mole fractions of GMO in the lipid mixture and the cmc of pure GMO, respectively. Based on the above assumptions, the monomer concentration of GMO in the respective lipid mixtures in the hemolysis and lipid mixing (FRET) experiments was calculated and the result is plotted in Fig. 5. Note that the hemolysis and FRET experiments were conducted at substantially different total lipid (LCNP) concentration, i.e. the total lipid (LCNP) concentration was 2.5 wt% (or 25 mg/ml) after mixing with rat whole blood whereas the total lipid (LCNP) concentration in the FRET experiment was 0.003 wt% (or 30 μg/ml). As shown in Fig. 5, despite the almost 3 orders of magnitude difference in total lipid (LCNP) concentration, the trends observed in the hemolysis and lipid mixing experiments are the same with a significant "effect onset" at a calculated GMO monomer concentration of about 2-3 μM. This indicates that it is the GMO monomer concentration

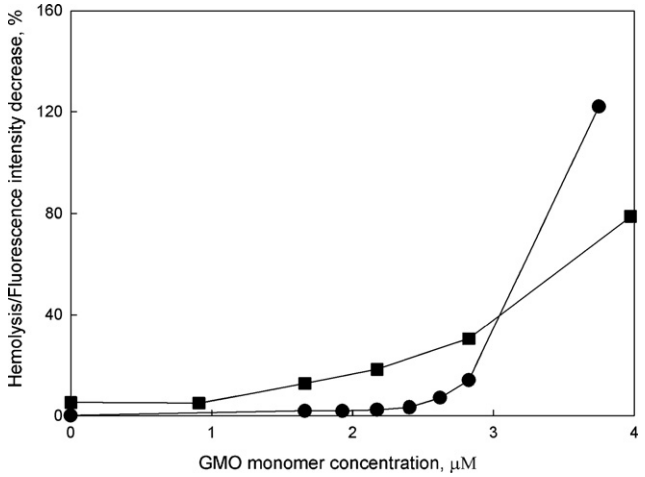

Fig. 5. Dependence of hemolysis (circles) and lipid mixing (in terms of fluorescence intensity decrease) (squares) on the estimated GMO monomer concentration in mixed systems of SPC/GDO/GMO/P80 (Table 1). Values taken for the zero GMO concentration correspond to the SPC/GDO/P80 LCNPs whereas the highest hemolysis value is taken from the GMO/P80 (80/20 wt/wt) LCNPs and the highest lipid mixing or intensity decrease value is taken from GMO/F127 (80/20 wt/wt) LCNPs.

that facilitates the interaction with rat RBCs and SPC multilamellar liposomes rather than direct particle–particle interactions (or fusion).

To support the conclusion of GMO monomer driven interaction with lipid membranes an additional experiment was performed where LCNPs based on GMO/F127 (90/10 wt/wt) were mixed with either plain SPC or with SPC/PEG-lipid unilamellar liposomes including 16 wt% (or ca 5 mol%) PEG-lipid (DOPE–PEG(2000)) in the latter composition. Because the presence of PEG-lipids in the lipid membrane is expected to effectively reduce particle–particle interactions through steric stabilization (Kenworthy et al., 1995; Čeh et al., 1997; Johnsson and Edwards, 2003), there should be a change in the lipid mixing kinetics if particle fusion is the driving force for the interaction rather than monomer exchange. As shown in Fig. 6, the lipid mixing kinetics were essentially identical for plain SPC and SPC/PEG-lipid liposomes thus again indicating GMO monomer exchange to be the most important factor.

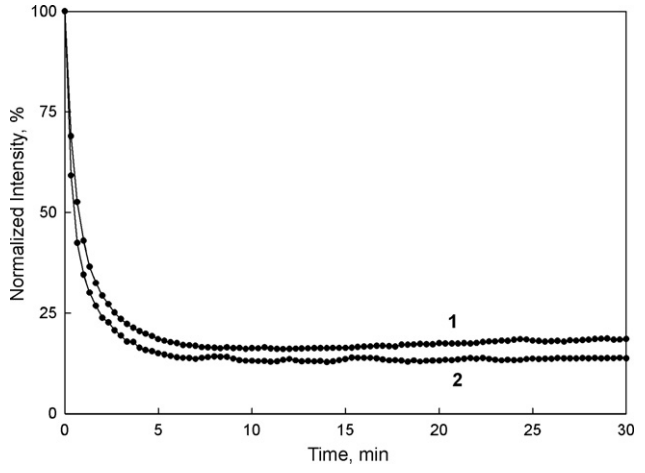

Fig. 6. FRET fluorescence intensity decays upon mixing of SPC (1) and SPC/PEG-lipid (84/16 wt/wt) (2) unilamellar liposomes with fluorescently labeled (NBD-PE and *N*-Rh-PE) GMO/F127 (90/10 wt/wt). The excitation wavelength was 463 nm and the emission intensity was recorded at 580 nm.

Interestingly, unsaturated monoglycerides such as GMO have been shown to exert high antiviral activity towards enveloped viruses (Sands et al., 1979) whereas the saturated counterparts were found to be inactive. The concentration of GMO needed for 50% inactivation of herpes simplex virus (HSV-2) was found to be about 1 μM, i.e. below the cmc_{GMO} of 4 μM, again indicating the importance of the monomer concentration for "membrane activity". Importantly, in the study by Sands et al., it was shown that by mixing GMO (or monoolein) with either GDO (diolein) or PC, the GMO-induced inactivation of two types of bacteriophages was essentially inhibited showing that both GDO and PC acted as to reduce GMO antiviral activity by lowering the GMO monomer activity in the mixed system. We also note that human plasma levels of *total* monoacyl glycerols (MAGs), of which an unknown fraction is unsaturated MAGs including GMO, are generally <1% of the total level of acylglycerols (MAGs, diacyl glycerols (DAGs) and triacyl glycerols (TAGs)) and that the fasted state MAG plasma levels are in the order of 2–5 μM (Fielding et al., 1993). Thus, the total MAG and therefore GMO plasma levels (and other unsaturated MAGs) are naturally kept relatively low which is obviously physiologically important given the high membrane destabilizing activity of GMO.

It appears clear from the above that the monomer concentration of the respective lipid or surfactant dispersion/solution is important for the hemolytic activity. However, this is obviously not the only factor as for example GMO and P80 have approximately the same cmc but cause significantly different levels of hemolysis. Another important factor is the structural impact of the incorporation of the particular lipid/surfactant into the cellular membrane. Taking GMO and P80 as examples, the former lipid is a cubic phase forming lipid whereas the latter is a "normal" micelle forming surfactant. Clearly, the cubic phase forming GMO has more pronounced membrane destabilizing effects and this may be related to potential phase segregation within the cell membrane introducing pore structures and resulting in leakage of the cellular content. This type of pore formation may also occur in normal surfactant/lipid membrane system (Edwards and Almgren, 1992) but, depending on the molecular nature of the surfactant, is generally not causing highly leaky lipid membranes until a relatively high fraction of the surfactant is present in the lipid bilayer. Hence, in addition to chemical activity, the local effect of a lipid or surfactant drug delivery vehicle constituent on cell membrane structural properties appears to play a role for its hemolytic activity and its ultimate qualification as drug delivery agent.

4. Conclusions

It is concluded that dispersed LCNPs based on SPC/GDO display very limited lipid mixing with SPC model membranes and practically no hemolysis when added to rat whole blood. The latter property is a pre-requisite for a drug delivery system intended for intravenous administration at higher exposures. In contrast, GMO-based LCNPs exhibit very fast and effective lipid mixing with phospholipid bilayers, both with model and cell membranes, resulting in, e.g. massive hemolysis when mixed with red blood cells. Partly this difference may be explained by difference in chemical activity, but the impact on bilayer membrane structure, e.g. of the cell also plays a role.

It is further concluded that there is a relatively good correlation between FRET lipid mixing experiments using model PC membranes (multilamellar liposomes) and *in vitro* hemolysis effects. Thus, dispersions resulting in a small degree of hemolytic activity *in vitro* also show limited lipid mixing with SPC bilayers. FRET experiments may therefore be used as one screening tool for the selection of viable lipid formulations for parenteral drug delivery and in particular for formulations intended for intravenous administration.

Acknowledgements

This work was supported by a grant from the Swedish Agency for Innovation Systems (VINNOVA), and the Camurus Lipid Research Foundation (Lund, Sweden). J. Barauskas acknowledges State Scholarship Award from the Lithuanian Ministry of Education and Science. M. Špandyreva and K. Ribokaitė acknowledge Student Research Fellowship Awards from the Lithuanian Science Council.

References

Barauskas, J., Johnsson, M., Joabsson, F., Tiberg, F., 2005a. Cubic phase nanoparticles (Cubosome®): principles for controlling size, structure & stability. Langmuir 21, 2569–2577.

Barauskas, J., Johnsson, M., Tiberg, F., 2005b. Self-assembled lipid superstructures: beyond vesicles and liposomes. Nano Lett. 5, 1615–1619.

Barauskas, J., Misiunas, A., Gunnarsson, T., Tiberg, F., Johnsson, M., 2006. "Sponge" nanoparticle dispersions in aqueous mixtures of diglycerol monooleate, glycerol dioleate and polysorbate 80. Langmuir 22, 6328–6334.

Barauskas, J., Nylander, T., 2008. Lyotropic liquid crystals as delivery vehicles for food ingredients. In: Garti, N. (Ed.), Delivery and Controlled Release of Bioactives in Foods and Neutraceuticals. Woodhead Publishing Ltd., Cambridge, pp. 107–131.

Barauskas, J., Cervin, C., Tiberg, F., Johnsson, M., 2008. Structure of lyotropic self-assembled lipid nonlamellar liquid crystals and their nanoparticles in mixtures of phosphatidylcholine and α-tocopherol (vitamin E). Phys. Chem. Chem. Phys. 10, 6483–6485.

Boyd, B.J., Whittaker, D.V., Khoo, S.-M., Davey, G., 2006. Lyotropic liquid crystalline phases formed from glycerate surfactants as sustained release drug delivery systems. Int. J. Pharm. 309, 218–226.

Čeh, B., Winterhalter, M., Frederik, P.M., Vallner, J.J., Lasic, D.D., 1997. Stealth liposomes; from theory to product. Adv. Drug Deliv. Rev. 24, 165–177.

Cervin, C., Vandoolaeghe, P., Nistor, C., Tiberg, F., Johnsson, M., 2009. A combined *in vitro* and *in vivo* study on the interactions between somatostatin and lipid-based liquid crystalline drug carriers and bilayers. Eur. J. Pharm. Sci. 36, 377–385.

Chen, M.-L., 2008. Lipid excipients and delivery systems for pharmaceutical development: a regulatory perspective. Adv. Drug Deliv. Rev. 60, 768–777.

Drummond, C.J., Fong, C., 2000. Surfactant self-assembly objects as novel drug delivery vehicles. Curr. Opin. Colloid Interface Sci. 4, 449–456.

Edwards, K., Almgren, M., 1992. Surfactant-induced leakage and structural change of lecithin vesicles: effect of surfactant headgroup size. Langmuir 8, 824–832.

Fielding, B.A., Humphreys, S.M., Allman, R.F.C., Frayn, K.N., 1993. Mono-, di- and triacylglycerol concentrations in human plasma: effects of heparin injection and of a high-fat meal. Clin. Chim. Acta 216, 167–173.

Gustafsson, J., Ljusberg-Wahren, H., Almgren, M., Larsson, K., 1997. Submicron particles of reversed lipid phases in water stabilized by nonionic amphiphilic polymer. Langmuir 13, 6964–6971.

Ho, S.-Y., Storch, J., 2001. Common mechanism of monoacylglycerol and fatty acid uptake by human intestinal Caco-2 cells. Am. J. Physiol. Cell Physiol. 281, 1106–1117.

Hyde, S.T., Andersson, S., Ericsson, B., Larsson, K., 1984. A cubic structure consisting of a lipid bilayer forming an infinite periodic minimum surface of the gyroid type in the glycerolmonooleate–water system. Z. Crystallogr. 168, 213–219.

Johnsson, M., Edwards, K., 2003. Liposomes, disks, and spherical micelles: aggregate structure in mixtures of gel phase phosphatidylcholines and poly(ethylene glycol)–phospholipids. Biophys. J. 85, 3839–3847.

Johnsson, M., Lam, Y., Barauskas, J., Tiberg, F., 2005. Aqueous phase behavior and dispersed nanoparticles of diglycerolmonooleate/glyceroldioleate mixtures. Langmuir 21, 5159–5165.

Johnsson, M., Barauskas, J., Norlin, A., Tiberg, F., 2006. Physicochemical and drug delivery aspects of lipid-based liquid crystalline nanoparticles: a case study of intravenously administered propofol. J. Nanosci. Nanotechnol. 6, 3017–3024.

Kenworthy, A.K., Hristova, K., Needham, D., McIntosh, T.J., 1995. Range and magnitude of the steric pressure between bilayers containing phospholipids with covalently attached poly(ethylene glycol). Biophys. J. 68, 1921–1936.

Larsson, K., 2000. Aqueous dispersions of cubic lipid–water phases. Curr. Opin. Colloid Interface Sci. 5, 64–69.

Larsson, K., Quinn, P., Sato, K., Tiberg, F., 2006. Lipids: Structure Physical Properties and Functionality, vol. 19. The Oily Press, Bridgwater.

Lee, K.W.Y., Nguyen, T.-H., Hanley, T., Boyd, B.J., 2009. Nanostructure of liquid crystalline matrix determines in vitro sustained release and in vivo absorption kinetics for hydrophilic model drugs. Int. J. Pharm. 365, 190–199.

Leesajakul, W., Nakano, M., Taniguchi, A., Handa, T., 2004. Interaction of cubosomes with plasma components resulting in the destabilization of cubosomes in plasma. Colloids Surface B 34, 253–258.

Ljusberg-Wahren, H., Nyberg, L., Larsson, K., 1996. Dispersion of the cubic liquid crystalline phase—structure, preparation, and functionality aspects. Chim. Oggi 14, 40–43.

Lutton, E.S., 1965. Phase behaviour of aqueous systems of monoglycerides. J. Am. Oil Chem. Soc. 42, 1068–1070.

Luzzati, V., Husson, F., 1962. The structure of the liquid-crystalline phases of lipid–water systems. J. Cell Biol. 12, 207–219.

Malmsten, M., 2007. Phase transformations in self-assembly systems for drug delivery applications. J. Dispers. Sci. Technol. 28, 63–72.

Miwa, A., Ishibe, A., Nakano, M., Yamahira, T., Itai, S., Jinno, S., Kawahara, H., 1998. Development of novel chitosan derivatives as micellar carriers of taxol. Pharm. Res. 15, 1844–1850.

Qiu, H., Caffrey, M., 2000. The phase diagram of the monoolein/water system: metastability and equilibrium aspects. Biomaterials 21, 223–234.

Salentinig, S., Yaghmur, A., Guillot, S., Glatter, O., 2008. Preparation of highly concentrated nanostructured dispersions of controlled size. J. Colloid Interface Sci. 326, 211–220.

Sands, J., Auperin, D., Snipes, W., 1979. Extreme sensitivity of enveloped viruses, including herpes simplex, to long-chain unsaturated monoglycerides and alcohols. Antimicrob. Agents Chemother. 15, 67–73.

Spicer, P.T., 2005. Progress in liquid crystalline dispersions: cubosomes. Curr. Opin. Colloid Interface Sci. 10, 274–279.

Strickley, R.G., 2004. Solubilizing excipients in oral and injectable formulations. Pharm. Res. 21, 201–230.

Struck, D.K., Hoekstra, D., Pagano, R.E., 1981. Use of resonance energy transfer to monitor membrane fusion. Biochemistry 20, 4093–4099.

Tanford, C., 1991. The Hydrophobic Effect: Formation of Micelles and Biological Membranes, 2nd ed. Krieger Publishing Company, Florida.

Thorsteinsson, M.V., Richter, J., Lee, A.L., DePhillips, P., 2005. 5-Dodecanoylaminofluorescein as a probe for the determination of critical micelle concentration of detergents using fluorescence anisotropy. Anal. Biochem. 340, 220–225.

Um, J.Y., Chung, H., Kim, K.S., Kwon, I.C., Jeong, S.Y., 2003. In vitro cellular interaction and absorption of dispersed cubic particles. Int. J. Pharm. 253, 71–80.

Vandoolaeghe, P., Barauskas, J., Johnsson, M., Tiberg, F., Nylander, T., 2009a. Interaction between lamellar (vesicles) and nonlamellar lipid liquid-crystalline nanoparticles as studied by time-resolved small-angle X-ray diffraction. Langmuir 25, 3999–4008.

Vandoolaeghe, P., Renie, A.R., Campbell, R.A., Nylander, T., 2009b. Neutron reflectivity studies of the interaction of cubic-phase nanoparticles with phospholipid bilayers of different coverage. Langmuir 25, 4009–4020.

Yaghmur, A., Glatter, O., 2009. Characterization and potential applications of nanostructured aqueous dispersions. Adv. Colloid Interface Sci. 147–148, 333–342.